OPTICS

Light amplification by seeded Kerr instability

G. Vampa,[1,2]*† T. J. Hammond,[1]† M. Nesrallah,[1] A. Yu. Naumov,[3] P. B. Corkum,[1,3] T. Brabec[1]*

Amplification of femtosecond laser pulses typically requires a lasing medium or a nonlinear crystal. In either case, the chemical properties of the lasing medium or the momentum conservation in the nonlinear crystal constrain the frequency and the bandwidth of the amplified pulses. We demonstrate high gain amplification (greater than 1000) of widely tunable (0.5 to 2.2 micrometers) and short (less than 60 femtosecond) laser pulses, up to intensities of 1 terawatt per square centimeter, by seeding the modulation instability in an $Y_3Al_5O_{12}$ crystal pumped by femtosecond near-infrared pulses. Our method avoids constraints related to doping and phase matching and therefore can occur in a wider pool of glasses and crystals even at far-infrared frequencies and for single-cycle pulses. Such amplified pulses are ideal to study strong-field processes in solids and highly excited states in gases.

Amplification of mode-locked laser pulses typically proceeds through linear optical pumping of a gain medium followed by stimulated emission at lower photon energies than that of the pump. The medium stores the energy difference, and material damage limits the maximum amplified power. Recently, the quest for ever higher-average powers and broader wavelength tunability has resulted in the exploitation of optical parametric amplification (*1*, *2*)—a second-order nonlinearity in which pump photons are split into pairs of conjugate lower-energy photons, without energy stored in the nonlinear crystal. However, phase matching and absorption of the pump and seed waves limits the center wavelength and the bandwidth of the amplified waves (*3*, *4*). Improving phase matching and transparency requires intense development of new nonlinear crystals. We show that Kerr instability (*5*–*7*), a third-order optical nonlinearity resulting in an intensity-dependent refractive index and common to any material, can compete with the more exploited parametric amplification.

The nonlinear Schrödinger equation with a Kerr third-order nonlinearity admits unstable solutions (*6*, *7*); pumping a nonlinear medium with a sufficiently intense driver leads to weak waves that experience exponential gain as they propagate. When these weak waves are seeded from noise, the continuous wave breaks up into an unstable train of pulses (*6*, *8*), leading to the disintegration of the spatial mode of an optical beam (*9*) or the formation of oceanic (*10*) and optical rogue waves (*11*). Despite the wide occurrence of Kerr instabilities in physics, the theoretical understanding is still limited to instabilities at frequencies comparable with that of the pump (*6*). Recently, a fully analytical theory of Kerr instabilities valid for perturbations of arbitrary frequencies has been developed (*7*) that predicts appreciable gain over a broad spectral range between about zero and twice the pump frequency. Here, we experimentally demonstrate seeded amplification of femtosecond laser pulses in the visible and infrared spectral regions.

By seeding gain at different wavelengths, it is possible to amplify femtosecond laser pulses over more than an octave bandwidth (Fig. 1). A comparison is shown for seed spectra at three different central wavelengths (0.6, 1.4, and 1.8 μm) (Fig. 1, pale colored solid lines) with the corresponding amplified spectra (Fig. 1, bright colors, solid lines). The gain medium is a $Y_3Al_5O_{12}$ (YAG) crystal pumped by long femtosecond pulses from a Ti:sapphire laser. Gain in excess of 1000 is achieved throughout the whole bandwidth spanning 0.5 to 2.2 μm by simply adjusting the angle θ (Fig. 1) between the seed and the pump beams. Not only can the gain be tuned to the desired wavelength, but the spectral bandwidth is also rather large. At 1.4 μm, for example, the 100-nm bandwidth of the seed is fully amplified. Despite the strong nonlinearity and the complex propagation of the pump through the crystal, the seed pulses propagate and amplify without appreciable phase modulation. We measured the amplified pulses with second-harmonic frequency resolved optical gating (SH-FROG). As demonstrated in Fig. 1, insets A to D, the duration of the amplified pulses remains close to the transform limit of the seed, in any case <60 fs, and can even be shorter than the seed by pumping with short pulses (fig. S3). Furthermore, the beam quality is preserved during amplification (fig. S1). Our newly developed theory suggests that single-cycle pulses can potentially be amplified by controlling the pump and seed wavelengths. Therefore, together with automatic phase matching demonstrated below, Kerr amplification offers an interesting new approach to amplifying single-cycle pulses in the visible (*12*, *13*), infrared (*14*–*16*), and even multicycle pulses in the terahertz region (*17*), where amplification schemes are presently nonexistent.

To characterize the gain, in the mathematical limit of continuous-wave seed and pump beams and infinitely extended in space, the amplification

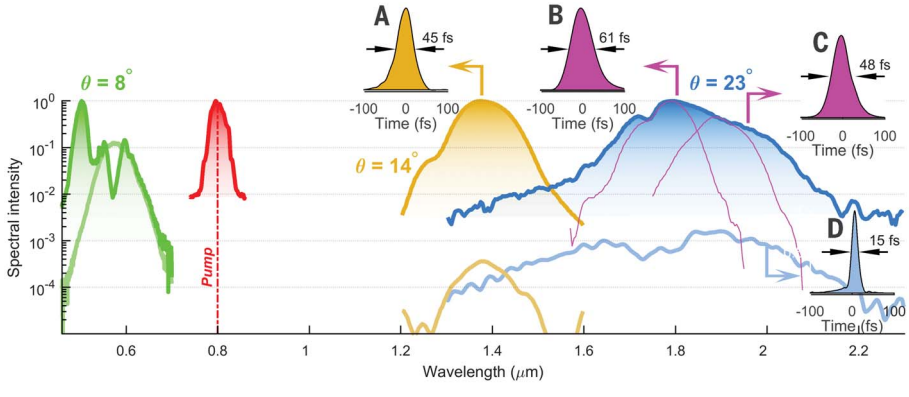

Fig. 1. Amplified spectra and pulse durations. Experimental amplified spectra (bright colors) and seed spectra (pale colors) for amplification around 0.5 μm (green), 1.4 μm (yellow), and 1.8 μm (blue), normalized to corresponding amplified spectra. The pump spectrum at 0.8 μm is shown in red. The angle between the pump and the seed laser beams (θ) is reported close to each amplified spectra. The pulse durations measured with a SHG-FROG are plotted in the insets for amplification spectra centered at (**A**) 1.4 μm, (**B**) 1.75 μm, and (**C**) 1.95 μm and (**D**) for the seed at 1.8 μm. The amplified pulses at 1.4 μm preserve the seed pulse duration of 45 fs [inset (A)]. Although the 1.8-μm seed pulses last only 15 fs (close to transform limit), the angular chirp of the amplification process narrows the spectrum that enters the FROG apparatus, which is positioned a few meters away from the YAG crystal. The measured spectra associated with insets (B) and (C) are plotted with purple lines. Each slice of the spectrum generates transform limited pulses (at 1.75 μm the measured bandwidth is 76 nm, and at 1.85 μm it is 100 nm).

[1]Department of Physics, University of Ottawa, Ottawa, ON K1N 6N5, Canada. [2]Stanford PULSE Institute, SLAC National Accelerator Laboratory, Menlo Park, CA 94025, USA. [3]National Research Council of Canada, Ottawa, ON K1A 0R6, Canada.
*Corresponding author. Email: gvampa@stanford.edu (G.V.); thomas.brabec@uottawa.ca (T.B.) †These authors contributed equally to this work.

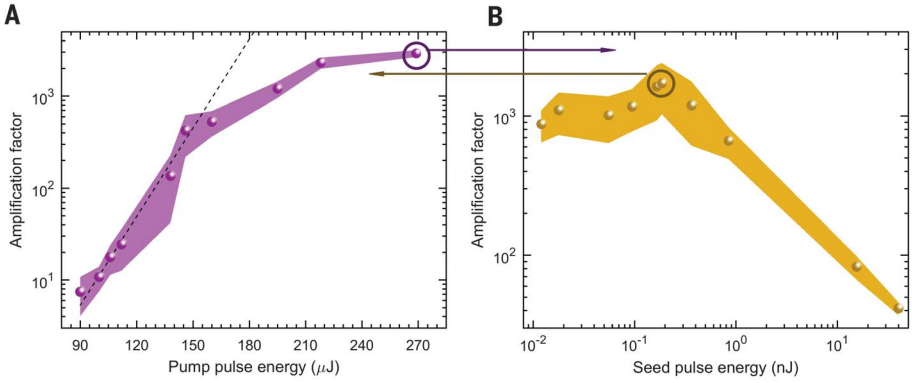

Fig. 2. Dependence of gain on pump and seed powers. (**A**) The amplification factor (the ratio between amplified and seed powers, spectrally integrated) increases exponentially with pump pulse energy, in agreement with theoretical expectation (black dotted line, which is reported in the supplementary materials) (*18*), but saturates for pump energies higher than 150 μJ, which are close to the damage threshold of YAG (~300 μJ, corresponding to a vacuum intensity of 10 TW/cm^2). (**B**) As a function of seed pulse energy, amplification remains high (>1000) for seed energies <0.2 nJ but decreases with a polynomial behavior for higher seed energies. Seed energy is varied at the maximum pump power (purple circles), whereas pump energy is varied at the seed energy just before the onset of saturation (yellow circle). The seed center wavelength is 1.4 μm.

Fig. 3. Angular chirp of the amplified spectrum. Amplified spectrum centered around 1.8 μm as a function of propagation angle, measured in the far field. The angular chirp of 3 μm/rad and the emission angle agree with the theoretical prediction (gray dashed line). It is the angularly integrated spectrum that is plotted as a blue line in Fig. 1.

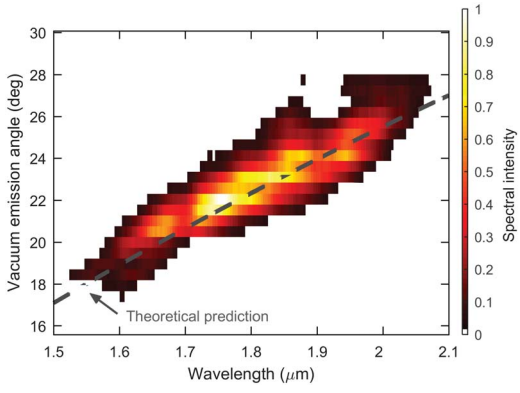

proceeds exponentially with the length of the crystal with intensity gain coefficient (*7*)

$$\bar{g}(\Omega) = \frac{k_{n(+)}k_{n(-)}}{\sqrt{k_p^2 - (\sigma D_u)^2}} \quad (1)$$

Here, $\Omega = \omega - \omega_p$ is the frequency shift between seed (ω) and pump (ω_p), $k_{n(\pm)}(\Omega) = (\omega_p \pm \Omega)\sqrt{n_2 I_p}/c$ is the nonlinear wavevector, and I_p and n_2 are the pump intensity and the nonlinear refractive index, respectively. $k_p^2 = k^2(\omega_p) + k_n^2(0)$ is the total wave vector of the pump given by adding the linear wave vector $k = \omega n(\omega)/c$ to the nonlinear wave vector at the pump wavelength. $\sigma = [k_v(\omega_p) + D_g]/k_p$, where $k_v^2(\omega) = k^2(\omega) + 2k_n^2(\omega)$ is the seed wave vector (the nonlinearity is added twice compared with k_p). $D_{\{g,u\}}$ takes into account the dispersion of the medium to any frequency shift (*7*). Amplification of finite pulses and Gaussian beams modifies this ideal gain factor by taking into account the temporal and spatial geometry (supplementary materials) (*18*).

We measured exponential growth with respect to pump intensity (Fig. 2A), in agreement with the theoretical prediction (Fig. 2A, dashed black line), up to saturation of the gain, which occurs close to the damage threshold of YAG. As a function of seed pulse energy (Fig. 2B), the gain remains constant up to 0.2 nJ and then also saturates. Saturation limits the amplified intensity to 1 TW/cm^2, which is ~10% of the pump intensity (the seed pulses are shorter than the pump, and the seed beam waist at the focus is smaller) (supplementary materials) (*18*). Near saturation, we observed cross-talk between the two similarly intense beams in the reduction of the speckle pattern generated by the pump beam. The maximum amplified energy is 1.6 μJ (from 40-nJ seed and 270-μJ pump), corresponding to an energy conversion efficiency of 0.6%. Chirped pulse amplification (*19*, *20*) can be used to increase the output energy.

We next demonstrated that phase matching still plays a role in Kerr amplification, as it does everywhere in nonlinear optics, by forcing different frequencies to propagate at slightly different directions, with angle $\theta = \sin^{-1}[\kappa_\perp/(k_p + \sigma D_u)]$ with respect to the pump beam. Here, $\kappa_\perp^2 = (k_p^2 - D_u^2)(\sigma^2 - 1)$ is the transverse momentum that experiences maximum gain. In contrast to conventional three- or four-wave mixing processes, however, here phase matching is automatically satisfied (*7*). The measured angular chirp (Fig. 3) matches the theoretical prediction well. Because the chirp is almost linear with wavelength, it will be possible to compensate for the beam divergence that phase matching imposes with a dispersive element placed just after the medium. Furthermore, the angular chirp is only weakly dependent on the pump intensity (fig. S6), suggesting that it is uniform across the amplified beam profile. Matching the transverse momentum of optimum gain is a critical parameter to achieve amplification. Optimum amplification of a desired wavelength is achieved in the experiment by tuning the angle θ (Fig. 1). And as confirmed in Fig. 3, the measured optimum angle coincides with that predicted by theory.

By using near-infrared pump pulses, we have demonstrated seeded amplification by means of Kerr instability of short femtosecond pulses over a widely tunable spectral range. Amplification occurred in a crystal (YAG) whose nonlinear refractive index is of average magnitude. The nonlinearity is at least 100 times stronger in special materials such as chalcogenide glasses (*21*) or graphene (*22*) or at frequencies at which the linear permittivity approaches zero (*23*). In the latter case, a total index change of 170% has been observed. Therefore, high gain amplification seems feasible in only a few micrometers, if not nanometers, of these materials, with gain coefficients as high as $\bar{g} \sim 100\ \mathrm{s\ mm^{-1}}$ (as opposed to ~ 5 mm^{-1}, as in YAG).

Our theory predicts that gain terminates at frequencies for which either $\kappa_\perp^2 < 0$ or $k_p^2 \simeq (\sigma D_u)^2$. In KBr pumped by 2.1-μm femtosecond pulses, the cut-off extends to 14 μm (~21 THz), and to 42 μm (~7.1 THz) in the CW limit, therefore up to far-infrared frequencies, at which nonlinear crystals perform poorly or amplification schemes are inexistent altogether. Neither linear gain media nor $\chi^{(2)}$ nonlinear crystals offer as wide a bandwidth tunability because of limitations in achieving phase matching (*4*) or because of narrow gain profiles. Several nonlinear crystals also absorb mid-infrared light (*24*).

The energy output can be scaled up to arbitrarily high energies by adapting chirped pulse amplification schemes (*19*, *20*). Furthermore, the amplified bandwidth can sustain single-cycle pulses. Therefore, Kerr amplification will result in a shift of design paradigm for next-generation high-intensity laser sources. For the moment, the demonstrated microjoule-level pulse energies are already suitable to trigger strong-field processes in condensed matter—such as high harmonic generation (*25*), ablation and damage (*26*), optically driven currents (*27*), and photoemission (*28*)—and to study highly excited Rydberg states (*29*).

Given the broad occurrence of Kerr nonlinear instabilities in nature (*10*, *11*), our demonstration with femtosecond laser pulses may prove useful to address the spatiotemporal evolution of instabilities in forms other than light over a broad range of frequencies, where the effect of the full linear and nonlinear (*23*) dispersion of the medium becomes important.

REFERENCES AND NOTES

1. R. Baumgartner, R. Byer, *IEEE J. Quantum Electron.* **15**, 432–444 (1979).
2. R. W. Boyd, *Nonlinear Optics* (Academic Press, 2003).
3. C. Manzoni, G. Cerullo, *J. Opt.* **18**, 103501 (2016).
4. B. E. Schmidt *et al.*, *Nat. Commun.* **5**, 3643 (2014).
5. K. Tai, A. Tomita, J. L. Jewell, A. Hasegawa, *Appl. Phys. Lett.* **49**, 236–238 (1986).
6. L. W. Liou, X. D. Cao, C. J. McKinstrie, G. P. Agrawal, *Phys. Rev. A* **46**, 4202–4208 (1992).
7. M. Nesrallah *et al.*, arXiv:1711.04417 [physics.optics] (2017).
8. K. Tai, A. Hasegawa, A. Tomita, *Phys. Rev. Lett.* **56**, 135–138 (1986).
9. D. Kip, M. Soljacic, M. Segev, E. Eugenieva, D. N. Christodoulides, *Science* **290**, 495–498 (2000).
10. C. Kharif, E. Pelinovsky, *Eur. J. Mech. B* **22**, 603–634 (2003).
11. J. M. Dudley, F. Dias, M. Erkintalo, G. Genty, *Nat. Photonics* **8**, 755–764 (2014).
12. E. Goulielmakis *et al.*, *Science* **320**, 1614–1617 (2008).
13. A. Wirth *et al.*, *Science* **334**, 195–200 (2011).
14. G. Krauss *et al.*, *Nat. Photonics* **4**, 33–36 (2010).
15. P. Krogen *et al.*, *Nat. Photonics* **11**, 222–226 (2017).
16. H. Liang *et al.*, *Nat. Commun.* **8**, 141 (2017).
17. M. Tonouchi, *Nat. Photonics* **1**, 97–105 (2007).
18. Materials and methods are available as supplementary materials.
19. D. Strickland, G. Mourou, *Opt. Commun.* **55**, 447–449 (1985).
20. A. Dubietis, G. Jonušauskas, A. Piskarskas, *Opt. Commun.* **88**, 437–440 (1992).
21. F. Smektala, C. Quemard, V. Couderc, A. Barthélémy, *J. Non-Cryst. Solids* **274**, 232–237 (2000).
22. H. Zhang *et al.*, *Opt. Lett.* **37**, 1856–1858 (2012).
23. M. Z. Alam, I. De Leon, R. W. Boyd, *Science* **352**, 795–797 (2016).
24. D. N. Nikogosyan, *Nonlinear Optical Crystals: A Complete Survey* (Springer Science & Business Media, 2006).
25. S. Ghimire *et al.*, *Nat. Phys.* **7**, 138–141 (2011).
26. R. R. Gattass, E. Mazur, *Nat. Photonics* **2**, 219–225 (2008).
27. A. Schiffrin *et al.*, *Nature* **493**, 70–74 (2013).
28. M. Krüger, M. Schenk, P. Hommelhoff, *Nature* **475**, 78–81 (2011).
29. U. Eichmann, A. Saenz, S. Eilzer, T. Nubbemeyer, W. Sandner, *Phys. Rev. Lett.* **110**, 203002 (2013).

ACKNOWLEDGMENTS

We acknowledge valuable financial support from the Air Force Office of Scientific Research (AFOSR) under award FA9550-16-1-0109, the AFOSR Multidisciplinary University Research Initiative grant FA9550-15-1-0037, and from Canada's National Research Council and Natural Sciences and Engineering Research Council. The authors declare no competing financial interests. G.V. thanks B. Schmidt for insightful discussions. All data needed to evaluate the conclusions in the paper are present in the paper and/or the supplementary materials.

SUPPLEMENTARY MATERIALS

www.sciencemag.org/content/359/6376/673/suppl/DC1
Materials and Methods
Supplementary Text
Figs. S1 to S6
References (*30*–*34*)

19 September 2017; accepted 21 December 2017
10.1126/science.aaq0053

Light amplification by seeded Kerr instability

G. Vampa, T. J. Hammond, M. Nesrallah, A. Yu. Naumov, P. B. Corkum and T. Brabec

Science **359** (6376), 673-675.
DOI: 10.1126/science.aaq0053

Seeding a laser amplifier

Amplification of femtosecond laser pulses requires a lasing medium or a nonlinear crystal. The chemical properties of the lasing medium or adherence to momentum conservation rules in the nonlinear crystal constrain the frequency and the bandwidth of the amplified pulses. Vampa *et al.* seeded modulation instability in a laser crystal pumped with femtosecond near-infrared pulses. This provided a method for the high gain amplification of broadband and short laser pulses up to intensities of 1 terawatt per square centimeter. The method avoids constraints related to doping and phase matching and can be expected to be applied to a wide pool of glasses and crystals.

Science, this issue p. 673